

## Configurational elastic energy in $\beta$ -brass

H. Kubo

*Research and Development Laboratories I, Central Research and Development Bureau, Nippon Steel Corporation,  
1618 Ida, Nakahara-ku, Kawasaki 211, Japan*

(Received 21 February 1984; revised manuscript received 26 April 1985)

An analytic expression for the configurational elastic energy (CEE) in ordered phases is derived using microscopic elasticity theory. Fourier methods are used to express the CEE for a given composition modulation in  $\mathbf{k}$  space. The theory is applied to a  $\beta$ -brass which has the  $B2$ -type ordered structure. Quantitative calculations are made on the CEE with use of the solute, solute-lattice, and lattice coupling parameters obtained from x-ray- and neutron-diffraction experiments. For a given Fourier component of composition modulation, the CEE in  $\mathbf{k}$  space exhibits spectra on two separate branches, which correspond to the optical mode and the acoustic mode of decomposition waves. Both modes of the CEE are found to exhibit strong orientation and wave-vector-magnitude dependence. Both modes have positive values at the special point  $(\frac{1}{2}, \frac{1}{2}, \frac{1}{2})$  but negative values at the  $\mathbf{k}$  space origin, which indicates that the CEE works to depress the  $DO_3$  ordering but also facilitates spinodal decomposition in the  $\beta$ -brass.

### I. INTRODUCTION

It is well known that coherency strains, which are caused by the size difference of the solute and the solvent atoms in alloy crystals, play an important role in the stability of alloy phases. For example, strain originating in the size difference of atoms makes the solid solution unstable and tends to facilitate decomposition.<sup>1</sup> Various calculations have been made on the elastic energies originating from the coherency strain. The microscopic elasticity theory is best known through its extensive use in calculating the elastic energies exhibited by the static displacements on defects.<sup>2-8</sup> The theory was first developed by Matsubara<sup>2</sup> and was greatly extended by Kanzaki<sup>3</sup> who calculated the displacements on substitutional atoms and vacancies in argon. After the work accomplished on point defects in crystals, the microscopic elasticity theory was applied to order-disorder transition<sup>9-14</sup> and omega<sup>15</sup> and other lattice (structural) transitions.<sup>16-18</sup> However, attention should be paid to the assumption involved in the theory that the elastic moduli or force constants of all the phases or defects participating in the decomposition process or pertinent to the structural transition are equal. This assumption is not strictly true in the case of cluster formation in solid solutions, because the relative difference in the elastic constants is of the order of  $10^{-2}$ . On the other hand, this is especially significant for the order-disorder transition, because the elastic constants vary in proportion to the square of the long-range order ( $\eta$ ), and in the ordered phase of  $\eta=1$ , the elastic constants are an order of magnitude larger than that of the disordered phase.<sup>14,19,20</sup> Therefore, in ordered phases, the elastic energies should be estimated using the elastic constants which have different values from that in the disordered phase.

The formation of an ordered phase imposes an additional condition in formulating the microscopic elasticity theory. The appearance of ordered spots in reciprocal

space reduces the volume of the first Brillouin zone (BZ). As a consequence, each discrete point allowed in the first BZ should represent multiple (displacement or concentration) waves by the number of sublattices in the ordered phase. This additional condition makes the theoretical treatment intricate.

In this paper, we consider the configurational elastic energy (CEE) in ordered phases using microscopic elasticity theory. Of course, this can be applied to various problems of the ordered phase, but we pay attention only to the elastic energies accompanied by coherent clustering and continuous ordering in the ordered phase. Experimentally, those phenomena have already been recognized in many binary alloys such as Cu-Zn (Refs. 21 and 22), Fe-Al (Ref. 23), Fe-Be (Ref. 24), and Fe-Si (Refs. 26-28) systems. The  $\beta$ -brass (Cu-Zn system) is a particularly interesting system from the CEE point of view, because a variety of transitions have been observed under the influence of elastic energies<sup>15-22</sup> and because all the parameters necessary for calculating the CEE have been obtained by experiments.<sup>29,30</sup> The second purpose of this paper is, therefore, to calculate the CEE in a  $\beta$ -brass ( $B2$ -type ordered phase) and to consider the contribution of it to the phase stability.

An expression for the configurational elastic energy in ordered phases is given in Sec. II, where an analytical expression in Fourier form is derived in analogy to that of a solid solution. In Sec. III the elastic energies developed by the concentration waves with the wave vectors in the first Brillouin zone are estimated for the  $B2$  phase of Cu-Zn system. The contribution of the elastic energy to the clustering and to the continuous ordering is considered. A brief discussion is given in Sec. IV.

### II. REPRESENTATION OF ELASTIC FREE ENERGY IN THE ORDERED PHASE

The microscopic or crystal-lattice-statics theory of elasticity has been developed on solid solutions of metal al-

loys.<sup>2-8</sup> In this approach, the solute atom functions as a center of force which acts to displace the lattice around it, while the lattice displacement is in turn opposed by the elastic resistance of the lattice. The former is called the internal force and the latter is called the lattice force.

In the ordered phase, the crystal can be subdivided into sublattices. Atoms on a particular sublattice may be distinguished from those on another sublattice. Consequently, both the internal force and the lattice force depend upon the atom species and the sublattices on which the atom is located. Mechanical equilibrium can then be expressed in a matrix form in Fourier space as follows:

$$-\Psi^*(q)\underline{Q}(q)=\Phi(q)\underline{U}(q), \quad (1)$$

where  $q$  represents the allowed triplet numbers ( $q_1, q_2, q_3$ ) in the first BZ of the reciprocal-lattice space. The left-hand side of Eq. (1) represents the internal force and the right-hand side expresses the lattice force. The matrix  $\Psi^*(q)$ , which is an adjoint matrix of  $\Psi(q)$ , is a Fourier transform (FT) of solute-lattice coupling parameters (CP's) given in a matrix form; when the alloy consists of  $t$  species of atoms and contains  $N$  unit cells of the ordered structure, each containing  $Z$  atoms distinguished by the sublattice position  $\gamma$  in the unit cell,  $\Psi(q)$  is a  $(t-1)Z \times 3(t-1)Z$  matrix with elements

$$\begin{aligned} \psi_{\sigma\sigma'}^i(\gamma; \gamma' | q) \\ (i=1,2,3; \sigma, \sigma'=1,2, \dots, t-1; \gamma, \gamma'=1,2, \dots, Z), \\ \psi_{\sigma\sigma'}^i(\gamma; \gamma' | q) = \frac{1}{(m_{\sigma\gamma} m_{\sigma'\gamma'})^{1/2}} \sum_n \psi_{\sigma\sigma'}^i(n\gamma - \gamma') \\ \times \exp[i\mathbf{k}(q) \cdot \mathbf{x}(n\gamma - \gamma')], \end{aligned} \quad (2)$$

where  $m_{\sigma\gamma}$  is the mass of an atom of the  $\sigma$ th species on the  $\gamma$  sublattice. The solute-lattice CP's  $\psi_{\sigma\sigma'}^i(n\gamma - \gamma')$  represents the force which acts along the  $i$  direction from a solute atom  $\sigma$  at location  $\mathbf{x}(n\gamma)$  on an atom  $\sigma'$  at site  $\mathbf{x}(\gamma')$ . Hence, the internal force is expressed in terms of the product of the solute-lattice CP's and the concentration variance  $\tau_{\sigma}(n\gamma) - c_{\sigma\gamma}^0$ , where  $\tau_{\sigma}(n\gamma)$  is unity if the  $\sigma$ th atom is located at position  $\mathbf{x}(n\gamma)$  and otherwise it is zero,  $c_{\sigma\gamma}^0$  representing an average concentration of the  $\sigma$ th atom on the  $\gamma$  sublattice. On making the FT of the concentration variance, we obtain a  $(t-1)Z$ -dimensional column vector  $\underline{Q}(q)$  in Eq. (1) with elements  $Q_{\sigma}(\gamma | q)$ . In the right-hand side of Eq. (1) the FT of a dynamical matrix  $\Phi(q)$  is a  $3(t-1)Z \times 3(t-1)Z$  symmetric matrix with elements  $\phi_{\sigma\sigma'}^{ij}(\gamma; \gamma' | q)$  which is defined on the analogy of the definition of the solute-lattice coupling parameter  $\psi_{\sigma\sigma'}^i(\gamma; \gamma' | q)$ .  $\underline{U}(q)$  is a FT of the displacement vector  $\underline{u}(n\gamma)$  and is a  $3(t-1)Z$ -dimensional column vector (see the definition in Ref. 22).

Elastic free energy of the alloy can generally be expressed in a power series of  $Q_{\sigma}(\gamma | q)$  and  $\underline{U}_{\sigma}(\gamma | q)$ . Making a harmonic approximation of the elastic free energy with respect to the  $Q_{\sigma}(\gamma | q)$  and  $\underline{U}_{\sigma}(\gamma | q)$ , and imposing the mechanical equilibrium condition expressed in Eq. (1), we obtain the following expression of the total elastic free energy in the ordered phase:

$$E = \frac{N}{2Z} \sum_q \underline{Q}^*(q) \underline{E}(q) \underline{Q}(q), \quad (3a)$$

$$\underline{E}(q) = \underline{L}(q) - \underline{\Psi}(q) \Phi^{-1}(q) \underline{\Psi}^*(q), \quad (3b)$$

where  $\underline{L}(q)$  is a  $(t-1)Z \times (t-1)Z$  matrix with elements  $L_{\sigma\sigma'}(\gamma; \gamma' | q)$ , which are a FT of solute CP's  $L_{\sigma\sigma'}(n\gamma - \gamma')$ . The solute CP's represent the elastic energy to bring an atomic pair from the pure solute or solvent to their ideal location defined by the average lattice of the alloy.<sup>31</sup>

$$\begin{aligned} L_{\sigma\sigma'}(n\gamma - \gamma') = -\phi_{\sigma\sigma'}^{ij}(n\gamma - \gamma') x_k(n\gamma - \gamma') x_l(n\gamma - \gamma') (\eta_{\sigma\gamma, ik} + \eta_{\sigma'\gamma', ik}) \\ \times (\eta_{\sigma\gamma, jl} + \eta_{\sigma'\gamma', jl}) C_{iqls} / 8(C_{iqls} + C_{trqs}), \quad n\gamma \neq \gamma' \end{aligned} \quad (4a)$$

$$L_{\sigma\sigma}(0) = \sum_{\sigma'} \sum_n \sum_{\gamma} \sum_{\gamma'} L_{\sigma\sigma'}(n\gamma - \gamma'), \quad (4b)$$

where the implicit summation is indicated over the repeated suffixes  $i, j, k$ , and  $l$ .  $\eta_{\sigma\gamma, ij}$  is an expansion coefficient with respect to the concentration of the  $\sigma$ th solute atom defined on the  $\gamma$  sublattice and Vegard's law is assumed on all species of atoms. Then, the stress-free strain or eigenstrain  $\epsilon_{\sigma\gamma, ij}$  of the  $\sigma$ th solute atom is expressed in terms of the concentration variance as follows:

$$\epsilon_{\sigma\gamma, ij} = \eta_{\sigma\gamma, ij} [\tau_{\sigma}(n\gamma) - c_{\sigma\gamma}^0]. \quad (5)$$

From the definition of  $\underline{L}(q)$ ,  $\underline{\Psi}(q)$ ,  $\Phi(q)$ , and from the translational and the rotational invariance of  $\underline{E}(q)$  of Eq. (3b), we can readily prove that  $\underline{L}(q)$  and  $\Phi(q)$  are real matrices and  $\underline{\Psi}(q)$  is a purely imaginary one. Therefore, the elastic energy modulus  $\underline{E}(q)$  is real.

In order to make clear the physical significance of Eq. (3a), we rewrite it in the form derived by Khachatryan.<sup>5,6</sup> The term  $\underline{L}(q)$  in Eq. (3b) is expressed in terms of elastic constants using long-wavelength relations:

$$\begin{aligned} E = \frac{N\Omega}{8Z} \sum_{\sigma} \sum_{\sigma'} \sum_{\gamma} \sum_{\gamma'} C_{ijkl} (\eta_{\sigma\gamma, ik} + \eta_{\sigma'\gamma', ik}) (\eta_{\sigma\gamma, jl} + \eta_{\sigma'\gamma', jl}) c_{\sigma\gamma}^0 - \frac{N\Omega}{2Z} \sum_{\sigma} \sum_{\gamma} C_{ijkl} \eta_{\sigma\gamma, ik} \eta_{\sigma\gamma, jl} (c_{\sigma\gamma}^0)^2 \\ - \frac{N}{2Z} \sum_q \underline{Q}^*(q) [\underline{\Psi}(q) \Phi^{-1}(q) \underline{\Psi}^*(q)] \underline{Q}(q), \end{aligned} \quad (6)$$

where the following identities are used to derive the above equation:

$$\sum_q Q_\sigma(\gamma|q)Q_{\sigma'}^*(\gamma'|q) = m_{\sigma\gamma}[c_{\sigma\gamma}^0(1-\delta_{\sigma\sigma'}c_{\sigma'\gamma'}^0)\delta_{\gamma\gamma'}], \quad (7)$$

where  $\delta_{\gamma\gamma'}$  and  $\delta_{\sigma\sigma'}$  are Kronecker  $\delta$  functions.

Khachatryan has put the expansion coefficient  $\eta_{\sigma\gamma,ij}$  in Eq. (6) equal to the stress-free strain  $\epsilon_{\sigma\gamma,ij}$  because he considered a crystal of pure solvent atoms as the initial state of the system. Hence, in Eq. (5),  $c_{\sigma\gamma}^0$  should vanish and  $\eta_{\sigma\gamma,ij}$  becomes equal to the stress-free strain  $\epsilon_{\sigma\gamma,ij}$ . In that case, the first term in Eq. (6) is the elastic self-energy which is a simple sum of self- (stress-free strain) energies exerted by each solute atom in the solvent crystal and it would be observed if the atoms did not interact. The second term is the energy created by the elastic image force which arises from relaxation (expansion or contraction of volume) of the unconstrained crystal surface. The third one is a configuration-dependent term which results from the direct elastic interaction of solute atoms.

In treating the effect of elastic energy on the reconfiguration of atoms, one needs to consider only the direct pairwise interaction since the self-energy and image-force contributions are unchanged by the configuration of a fixed number of solute atoms. Taking into account the above mentioned, the total elastic energy  $E$  of Eq. (3a) is rewritten to represent the CEE explicitly in the following form:

$$E = \sum_\gamma \sum_{\gamma'} [E_0(\gamma;\gamma') + E_{\text{conf}}(\gamma;\gamma')], \quad (8a)$$

$$E_0(\gamma;\gamma') = \frac{N}{2Z} \sum_\sigma \sum_{\sigma'} m_{\sigma\gamma} [c_{\sigma\gamma}^0(1-\delta_{\sigma\sigma'}c_{\sigma'\gamma'}^0)\delta_{\gamma\gamma'}] \langle Z_{\sigma\sigma'}(\gamma;\gamma'|q) \rangle, \quad (8b)$$

$$E_{\text{conf}}(\gamma;\gamma') = \frac{N}{2Z} \sum_q \sum_\sigma \sum_{\sigma'} Q_\sigma(\gamma|q) [Z_{\sigma\sigma'}(\gamma;\gamma'|q) - \langle Z_{\sigma\sigma'}(\gamma;\gamma'|q) \rangle] Q_{\sigma'}^*(\gamma'|q), \quad (8c)$$

$$Z_{\sigma\sigma'}(\gamma;\gamma'|q) = L_{\sigma\sigma'}(\gamma;\gamma'|q) - \Psi_{\sigma\sigma'}(\gamma;\gamma'|q) \Phi_{\sigma\sigma'}^{-1}(\gamma;\gamma'|q) \Psi_{\sigma\sigma'}^*(\gamma;\gamma'|q), \quad (8d)$$

where submatrices  $\Psi_{\sigma\sigma'}(\gamma;\gamma'|q)$  and  $\Phi_{\sigma\sigma'}^{-1}(\gamma;\gamma'|q)$  are used for the convenience of explanation of the configurational part of the elastic energy in each sublattice system. The average  $\langle Z_{\sigma\sigma'}(\gamma;\gamma'|q) \rangle$  should be done over the wave vector  $\underline{k}(q)$  in the first BZ of the crystal. In Eq. (8c) when the distribution of solute atoms is perfectly random on the  $\alpha$  and  $\beta$  sublattice, the term  $Q_\sigma(\gamma|q)Q_{\sigma'}^*(\gamma'|q)$  does not depend on wave vector  $\underline{k}(q)$ , and then the CEE  $E_{\text{conf}}(\gamma;\gamma')$  vanishes in the disordered phase of the sublattice system  $(\gamma;\gamma')$ . On the other hand, the elastic energy  $E_0(\gamma;\gamma')$  always has a positive value which is brought about by the dissolution of solute atoms into the solvent matrix of the sublattice system  $(\gamma;\gamma')$ . It is instructed to indicate that  $\sum_\gamma \sum_{\gamma'} E_{\text{conf}}(\gamma;\gamma')$  is nearly equal to the negative value of  $\sum_\gamma \sum_{\gamma'} E_0(\gamma;\gamma')$  for the B2 phase of  $\eta=1$  in the equiatomic binary system. This comes from the fact that the nearest-neighbor pair of atoms in the B2 phase constitutes the standard state (no strain) configuration of a binary alloy, and then  $\sum_{\gamma\gamma'} [E_0(\gamma;\gamma') + E_{\text{conf}}(\gamma;\gamma')]$  is nearly equal to zero for the B2 phase of the binary system. Hence, the  $\sum_\gamma \sum_{\gamma'} E_0(\gamma;\gamma')$  term may be understood as the elastic driving force for the B2 ordering in the disordered B2 phase.

### III. CONFIGURATIONAL ELASTIC ENERGY IN A $\beta$ -BRASS

The quantitative calculation of the CEE has been made on the  $\beta$ -brass (Cu-38.9 at. % Zn) which has an ordered B2 structure. With the use of this calculation, Eq. (8c) can be expressed in a simple form as follows:

$$E_{\text{conf}} = \frac{N}{2Z} \sum_q \sum_\gamma \sum_{\gamma'} E_c(\gamma;\gamma'|q) Q(\gamma|q) Q^*(\gamma'|q), \quad (9a)$$

$$E_c(\gamma;\gamma'|q) = Z(\gamma;\gamma'|q) - \langle Z(\gamma;\gamma'|q) \rangle, \quad (9b)$$

where the summation over  $\gamma$  and  $\gamma'$  should be made on the two sublattices  $\alpha$  and  $\beta$ . The estimation of the CEE modulus will be made using the solute, solute-lattice, and lattice CP's. These values are listed in Table I, where the notation  $\alpha_{j\gamma}^i$  and  $\beta_j^i$  are used to represent the lattice coupling parameters after Gilat and Dolling.<sup>30</sup> The solute-lattice coupling parameters have been obtained by the present author from the analysis of x-ray diffuse scattering of the  $\beta$ -brass.<sup>29</sup> Out to third neighbors of atoms, three constants  $\hat{\alpha}_{\alpha\beta}^{(1)}$ ,  $\hat{\alpha}_{\beta\beta}^{(2)}$ , and  $\hat{\alpha}_{\beta\beta}^{(3)}$  were obtained and two

constants  $\hat{\alpha}_{\alpha\alpha}^{(2)}$  and  $\hat{\alpha}_{\alpha\alpha}^{(3)}$  have been left unknown. In performing the calculation,  $\hat{\alpha}_{\alpha\alpha}^{(2)}$  and  $\hat{\alpha}_{\alpha\alpha}^{(3)}$  are assumed to have the value  $-2.00 \times 10^{-12}$  N and zero, respectively. This comes from the experimental results obtained by Cook<sup>32</sup> and the present author<sup>29</sup> that in the disordered  $\beta$ -brass  $\hat{\alpha}_{\alpha\alpha}^{(2)} + 4\hat{\alpha}_{\alpha\alpha}^{(3)} = 3.39 \times 10^{-11}$  N, and in the ordered one  $\hat{\alpha}_{\beta\beta}^{(2)} + 4\hat{\alpha}_{\beta\beta}^{(3)} = 6.97 \times 10^{-11}$  N. The solute CP's are estimated from Eq. (4), where the expansion coefficients are assumed to be constant, i.e.,  $\eta_{\gamma\gamma',ij} = 0.068\delta_{ij}$ . Three sets of CEE  $E_c(\alpha;\alpha|q)$ ,  $E_c(\alpha;\beta|q)$ , and  $E_c(\beta;\beta|q)$  have been calculated on the discrete reciprocal points  $q$  separated from each other by  $(\Delta q) = (\frac{1}{500}, \frac{1}{500}, \frac{1}{500})$ . Figures 1(a)–1(f) show the view of the contours representing the CEE moduli,  $E_c(\gamma;\gamma'|q)$ 's in the first BZ of the (001)\* and the (110)\* reciprocal plane. In order to explain the physical meaning of the contour map, we consider the case in which the degree of order ( $\eta$ ) is unity in the present  $\beta$ -brass. For the Cu-38.9 at. % Zn alloy in B2

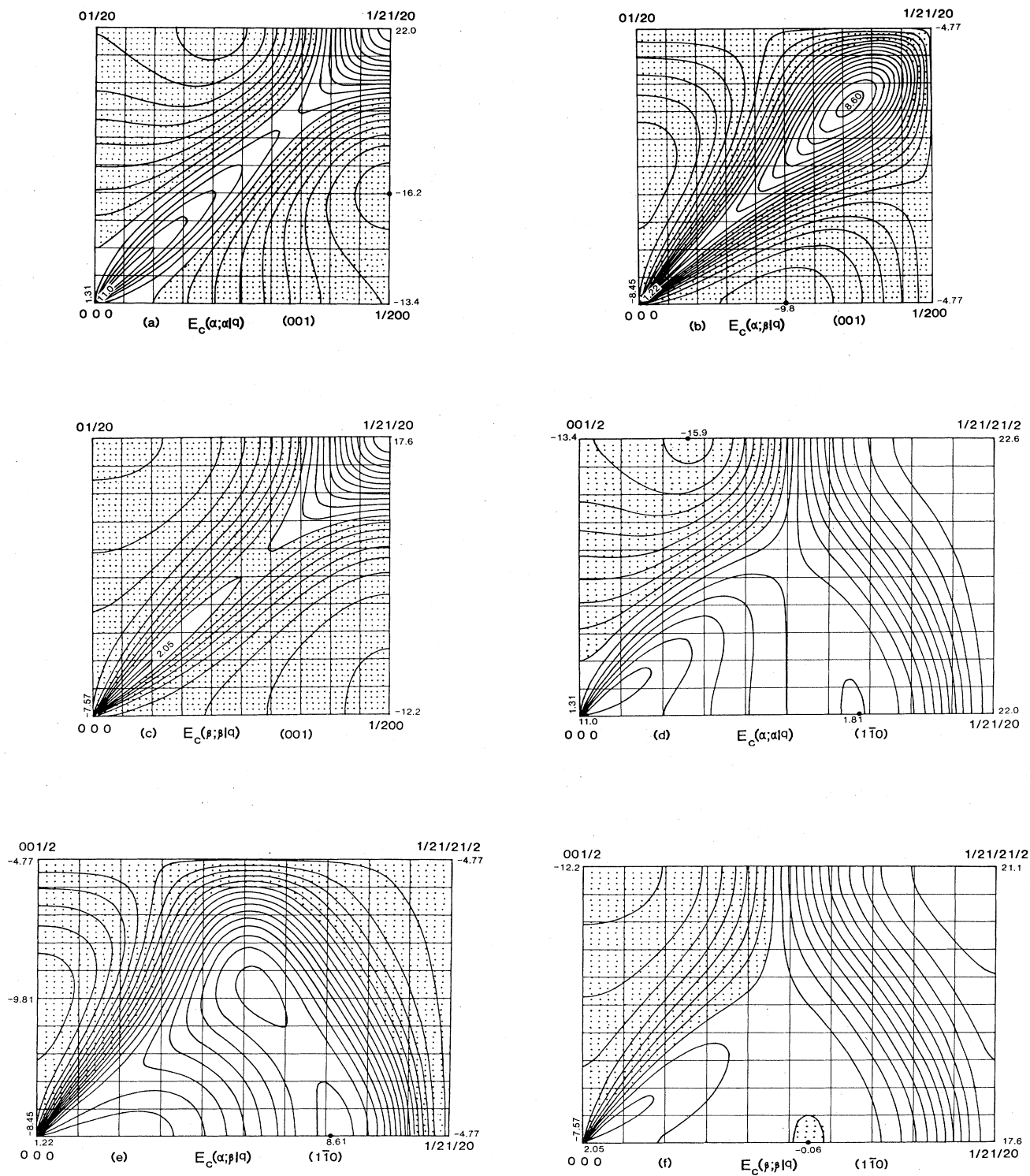


FIG. 1. Contours of configurational energy modulus  $E_c(\gamma; \gamma' | q)$  of  $\beta$ -brass (Cu-38.9 at. % Zn) in units of  $10^{-21}$  J/atom. The dots indicate the negative region of the CEE modulus. (a)  $E_c(\alpha; \alpha | q)$  in the (001)\* plane, (b)  $E_c(\alpha; \beta | q)$  in the (001)\* plane, (c)  $E_c(\beta; \beta | q)$  in the (001)\* plane, (d)  $E_c(\alpha; \alpha | q)$  in the (1 $\bar{1}$ 0)\* plane, (e)  $E_c(\alpha; \beta | q)$  in the (1 $\bar{1}$ 0)\* plane, and (f)  $E_c(\beta; \beta | q)$  in the (1 $\bar{1}$ 0)\* plane.

TABLE I. Numerical values used for the calculation of CEE in  $\beta$ -brass.  $\alpha_j^i$  and  $\beta_j^i$  are force constants.  $\hat{\alpha}_{\gamma\gamma}^{(i)}$  and  $\bar{\alpha}_{\gamma}^{(i)}$  are solute-lattice and solute coupling parameters, respectively. The elastic constants  $C_{ij}$ 's are those obtained by the ultrasonic method.

Lattice coupling parameter (model 4E) (N/m)	
$\alpha_1^1$	8.420
$\beta_1^1$	11.340
$\alpha_{10}^2$	7.110
$\alpha_{11}^2$	0.730
$\alpha_{10}^3$	1.070
$\alpha_{11}^3$	1.190
$\alpha_1^4$	0.280
$\alpha_2^4$	0.370
Solute-lattice coupling parameter ( $10^{-11}$ N)	
$\hat{\alpha}_{\alpha\beta}^{(1)}$	24.2
$\hat{\alpha}_{\alpha\alpha}^{(2)}$	-0.20
$\hat{\alpha}_{\beta\beta}^{(2)}$	2.97
$\alpha_{\alpha\alpha}^{(3)}$	0.0
$\hat{\alpha}_{\beta\beta}^{(3)}$	1.00
Solute coupling parameter ( $10^{-22}$ N m)	
$\bar{\alpha}_{\alpha\beta}^{(1)}$	26.66
$\bar{\alpha}_{\alpha\alpha}^{(2)}$	7.15
$\bar{\alpha}_{\beta\beta}^{(2)}$	0.74
$\bar{\alpha}_{\alpha\alpha}^{(3)}$	2.15
$\bar{\alpha}_{\beta\beta}^{(3)}$	2.39
$\bar{\alpha}_{\alpha\beta}^{(4)}$	1.96
Elastic constant <sup>a</sup> ( $10^{-11}$ N/m <sup>2</sup> )	
$C_{11}$	1.316
$C_{12}$	1.097
$C_{44}$	0.744
$\frac{1}{2}(C_{11}-C_{12})$	0.109
Atomic weight	
$m_{\text{Cu}}=63.54$	$m_{\text{Zn}}=65.38$
Lattice constant $a=0.2954$ (nm)	

<sup>a</sup>Y. Murakami and S. Kachi, Jpn. J. Appl. Phys. 13, 1728 (1974).

phase with  $\eta=1$ , all the  $\alpha$  sublattice points are occupied by Cu atoms. On the  $\beta$  sublattice, on the contrary, the solid solution is formed with the composition of Cu-77.8 at. % Zn. Therefore, the decomposition is possible only on the  $\beta$  sublattice. As a result, only the CEE  $E_c(\beta;\beta|q)$  has to be considered. A second assumption is that the free energy is entirely elastic. The estimated values shown in Figs. 1(c) and 1(f) reveal the pronounced characteristics

of orientation and wave-vector-magnitude dependence of the CEE modulus. The decomposition may occur at any point  $q$  which has negative CEE value. When the  $\langle 100 \rangle$ ,  $\langle 110 \rangle$ , and  $\langle 111 \rangle$  high-symmetry directions are considered, the decomposition takes place only along the  $\langle 100 \rangle$  directions which are elastically more soft than the other two directions. It also stands for the case that the free energy is taken into consideration, because only CEE exhibits the strong anisotropy with respect to the direction of  $\underline{k}(q)$ . This strong anisotropy is one of the characteristics of CEE in metals and alloys.<sup>1,7</sup> At early stages of decomposition, the decomposition wave grows in proportion to the exponential of the negative value of CEE.<sup>33</sup> Hence, among many points  $q$ , the decomposition may occur predominantly at the point  $q$  which has a minimum value of CEE, and the final phase which will be obtained by continuous ordering or continuous decomposition can be determined from the minimum point  $q$ . In the present case of  $\eta=1$ , it occurs at  $q=(\frac{1}{2}, 0, 0)$  or  $(0, \frac{1}{2}, 0)$  as shown in Fig. 1(c), which gives rise to the ordered phase of  $M=1$  with the second kind of antiphase domain vector in the B2 structure. It is to be recalled, however, that the above consequence is not derived by considering the total free energy but only from the CEE of the  $\beta$  sublattice of the  $\beta$ -brass.

It is evident from Eq. (9b) that the CEE is the difference in elastic free energy between the decomposed phase (cluster or ordered phase)  $Z(\gamma;\gamma'|q)$  and random solute distributions  $\langle Z(\gamma;\gamma'|q) \rangle$ . Cahn, on the other hand, has only shown explicitly the term  $Z(\gamma;\gamma'|q) = 2\Omega\eta^2 Y(\gamma;\gamma'|q)$  in his expression of the elastic energy, and as indicated by Cook and de Fontaine,<sup>7</sup> the term  $\langle Z(\gamma;\gamma'|q) \rangle$  is only included implicitly in the equation.<sup>1</sup> Therefore, in the expression used by Cahn in his continuum model, the elastic energy modulus always has a positive value, but in the present expression of the configurational elastic energy modulus, it may have either positive or negative value depending upon the relative magnitude of  $Z(\gamma;\gamma'|q)$  and  $\langle Z(\gamma;\gamma'|q) \rangle$ . It is to be noted that the average  $\langle Z(\gamma;\gamma'|q) \rangle$  always has a positive value since it represents the net elastic energy brought about by the random distribution of solutes in the stress-free solvent matrix. Therefore, the solid solution of the sublattice system is elastically favorable to be decomposed into incoherent (strain-free) phase.

Without any restriction on the amplitude of the decomposition wave, we have to consider the eigenvalues of the symmetric matrix  $\underline{E}_c(q)$  for obtaining the maximum and the minimum CEE in the alloy system. By using the estimated values of the elastic energy moduli  $E_c(\gamma;\gamma'|q)$ 's, the eigenvalues  $e(+)$  and  $e(-)$ , which are the maximum and the minimum CEE modulus, respectively, are obtained as a function of the wave vector  $\underline{k}(q)$ . The relation between the eigenvalues  $e(\pm)$  and the CEE moduli  $E_c(\gamma;\gamma'|q)$ 's can be readily understood from a drawing of the CEE contour in an amplitude space whose base axes are  $Q_\alpha$  and  $Q_\beta$ . Figure 2 shows a curved surface of the CEE for the decomposition wave with the wave vector  $\underline{k}(q)=\underline{k}(0.05, 0, 0)$ , which is taken into consideration as an example. The Cartesian coordinates  $Q_\alpha$  and  $Q_\beta$  in the figure represent the amplitudes of the decomposition

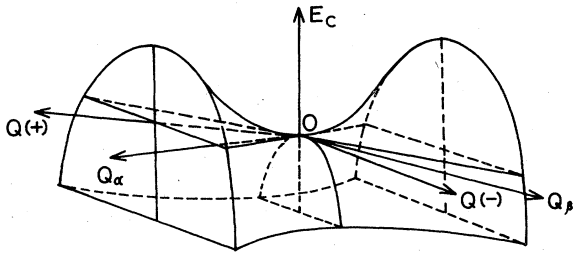


FIG. 2. Drawing of the CEE in amplitude space  $Q_\alpha - Q_\beta$ , where the concentration wave is assumed to have the wave vector  $\underline{k}(q) = k(0.05, 0, 0)$ . The tangents of the eigenvectors  $\underline{Q}(-)$  and  $\underline{Q}(+)$  are 1.13 and  $-0.99$  in the Cartesian coordinate  $Q_\alpha - Q_\beta$ , respectively.

waves. Because the CEE is drawn in a form  $\sum_\gamma \sum_{\gamma'} E_c(\gamma; \gamma' | q) Q(\gamma | q) Q^*(\gamma' | q)$  for the particular wave vector  $\underline{k}(q)$ , as shown in Eq. (9a), the modulus  $E_c(\gamma; \gamma' | q)$  represents the curvature of the surface in Fig. 2. For example, at  $(q) = (0.05, 0, 0)$  the cross section of the CEE surface is upwards concave along the  $Q_\alpha$  axis and is upwards convex along the  $Q_\beta$  axis. In fact the estimated elastic energy modulus  $E_c(\alpha; \alpha | q)$  has the positive value of  $1.0 \times 10^{-21}$  J/atom and the modulus  $E_c(\beta; \beta | q)$  has the negative value  $-7.7 \times 10^{-21}$  J/atom. From the estimated values of  $E_c(\alpha; \alpha | q)$ ,  $E_c(\alpha; \beta | q)$ , and  $E_c(\beta; \beta | q)$ , the eigenvalues can be obtained as  $e(+)=6.25 \times 10^{-21}$  J/atom and  $e(-)=-12.9 \times 10^{-21}$  J/atom. The corresponding eigenvectors can also be obtained and are shown in the figure as  $\underline{Q}(+)$  and  $\underline{Q}(-)$ , respectively. It is readily understood from the figure that the decomposition wave along  $\underline{Q}(-)$  grows up at the maximum speed in the system and decays most rapidly along  $\underline{Q}(+)$  direction.

Because the decomposition waves along the eigenvectors  $\underline{Q}(\pm)$  are composed of two basic waves  $Q_\alpha$  and  $Q_\beta$ , the growth or decay of the waves along  $\underline{Q}(\pm)$  signifies the concurrent growth or decay of the waves on the  $\alpha$  and the  $\beta$  sublattice. The amplitude ratio  $Q_\beta/Q_\alpha$  of the "eigenwave," which is identical to the tangents  $T(\pm)$  of the eigenvectors in the  $Q_\alpha - Q_\beta$  amplitude space, can be given by the following equation:

$$T(\pm) = 2E_c(\alpha; \beta | q) [E_c(\beta; \beta | q) - E_c(\alpha; \alpha | q) \pm \sqrt{D(q)}]^{-1}, \quad (10a)$$

$$D(q) = [E_c(\alpha; \alpha | q) - E_c(\beta; \beta | q)]^2 + 4[E_c(\alpha; \beta | q)]^2. \quad (10b)$$

It is straightforward from Eq. (10a) to specify the directions of eigenvectors  $\underline{Q}(\pm)$  in the  $Q_\alpha - Q_\beta$  amplitude space. That is, when the cross term  $E_c(\alpha; \beta | q)$  is positive, the eigenvector  $\underline{Q}(\pm)$  must be directed in the region  $Q_\alpha Q_\beta > 0$  and the eigenvector  $\underline{Q}(-)$  must be in the region  $Q_\alpha Q_\beta < 0$ . On the contrary, when  $E_c(\alpha; \beta | q)$  is negative, the opposite relation holds between the directions of  $\underline{Q}(\pm)$  and the sign of  $Q_\alpha Q_\beta$ . Thus, when only two sublattices are present in the crystal, the cross term of the CEE modulus determines the direction of the eigenvectors in the amplitude space. It is evident that one of the eigen-

values is always in the region  $Q_\alpha Q_\beta > 0$  and the other is always in the region  $Q_\alpha Q_\beta < 0$ . It signifies that there are two pairs of concentration waves with the same wave vector on the  $\alpha$  and  $\beta$  sublattice, and that one pair has the amplitudes with the same sign and the other has a different sign of the amplitudes. This conclusion derives the concept of phase angle between the decomposition waves. Because we consider many concentration waves on the two different sublattices  $\alpha$  and  $\beta$ , the phase difference can be considered between the two waves which have the same wave vector. For example, Fig. 3 shows the decomposition waves on the  $\alpha$  and  $\beta$  sublattice, where the phase is different by  $\pi$ , i.e.,  $Q_\alpha Q_\beta < 0$ . This mode of decomposition waves is, after the theory of lattice dynamics,<sup>33,34</sup> metaphorically called "optical mode of decomposition waves." On the other hand, if two waves have no phase difference, i.e.,  $Q_\alpha Q_\beta > 0$ , they are called "acoustic mode of decomposition waves." The theory of lattice dynamics insures that the difference of phase angle should be  $\pi$  for the optical mode of vibration waves and that it should be zero for the acoustic mode of vibration waves. The phase angle gradually changes with the wave vector from the origin to the point on the BZ boundary to have the value  $\pi/2$ . This is the same in the decomposition waves on the sublattices  $\alpha$  and  $\beta$ . Therefore, the situation that the phase angle is different by  $\pi$  as shown in Fig. 3 can be attained only in the limit of very long wavelength, i.e., in spinodal decomposition. To identify the decomposition modes of concentration waves corresponding to the maximum and the minimum eigenvalues  $e(+)$  and  $e(-)$ , respectively, the sign of the cross term  $E_c(\alpha; \beta | q)$  should be consulted with. For example, in the vicinity of the origin in Fig. 1(b), it has a negative value along the  $\langle 100 \rangle$  directions. Therefore, the eigenvectors corresponding to the maximum and the minimum CEE modulus must exist in the region  $Q_\alpha Q_\beta < 0$  and  $Q_\alpha Q_\beta > 0$  of Fig. 2, respectively. Thus, the maximum CEE modulus  $e(+)$  is attained by the optical mode of decomposition and the minimum one  $e(-)$  is obtained by the acoustic mode of decomposition. Figure 4 shows the view of the contours of the eigenvalues  $e(\pm)$  in the  $(001)^*$  reciprocal plane [Figs. 4(a) and 4(c)] and in the  $(110)^*$  reciprocal plane [Figs. 4(b) and 4(d)]. There are always two kinds of decomposition mode with respect to the same vector.

It is to be noted that if the decomposition took place in a disordered phase, the eigenvalue of the optical mode of decomposition could be drawn outside of the first BZ of

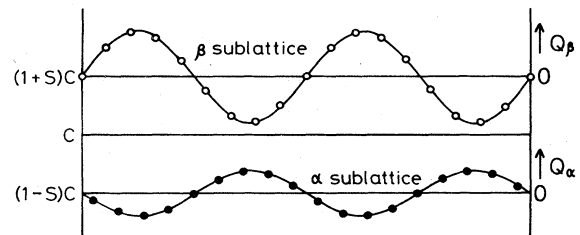


FIG. 3. Optical mode of long-wavelength decomposition. The two waves on the  $\alpha$  and the  $\beta$  sublattice have the same wavelength but have a different phase angle by  $\pi$ .

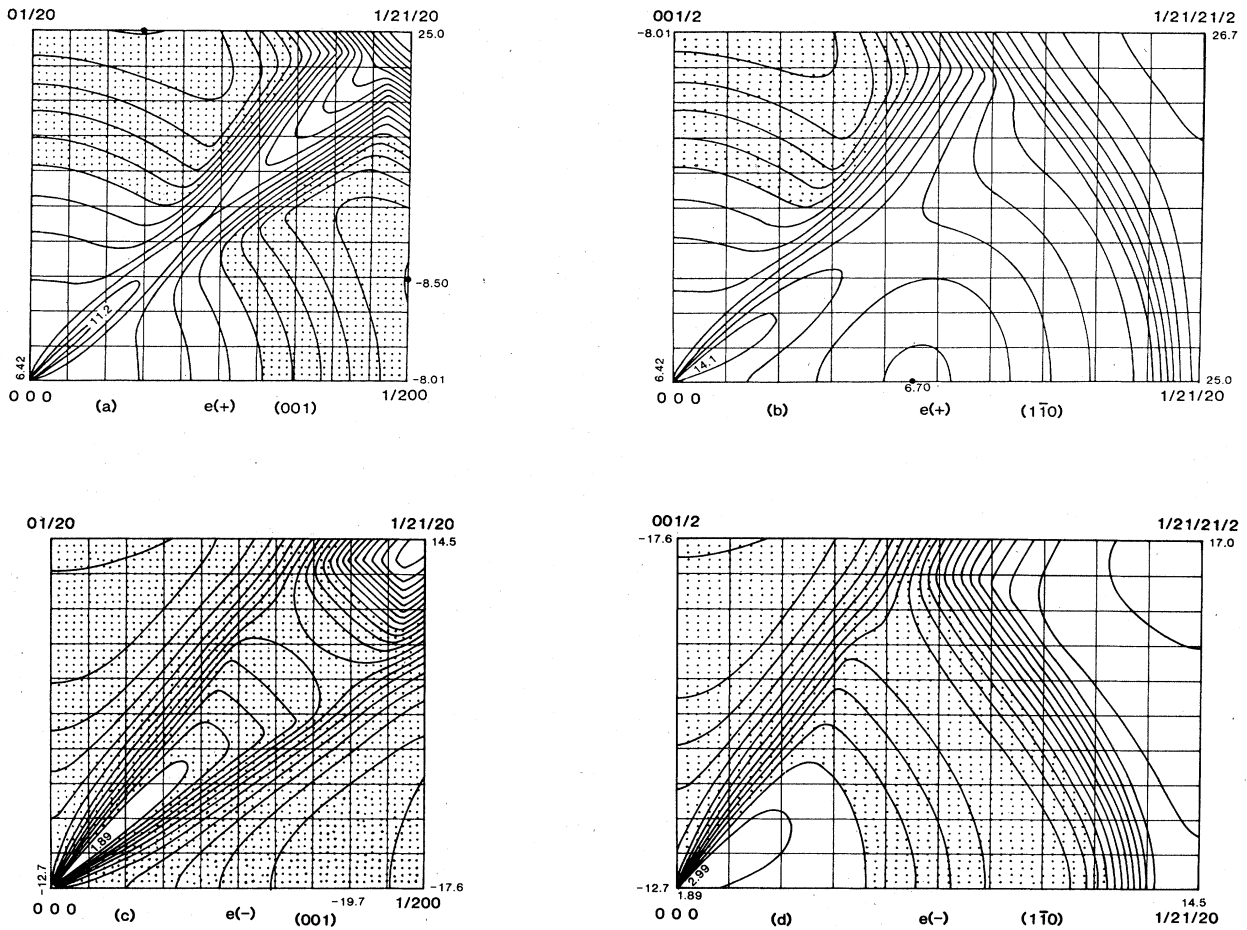


FIG. 4. Contours of the eigenvalues  $e(\pm)$  of the CEE matrix  $\underline{E}_c(q)$ , in units of  $10^{-21}$  J/atom. (a) and (b) show the maximum values,  $e(+)$ , in the  $(001)^*$  and  $(1\bar{1}0)^*$  plane, respectively. (c) and (d) show the minimum values,  $e(-)$ , in  $(001)^*$  and in  $(1\bar{1}0)^*$  plane, respectively.

the ordered phase by reflecting it with respect to the BZ boundary. Hence, the optical mode of decomposition waves with the long-wavelength limit  $|q|=0$  can be thought of as a sort of ordering wave. The one along  $[100]$  or  $[111]$  direction especially indicates a  $B2$  ordering wave. Therefore, the total CEE, i.e.,

$$E_c(\alpha; \alpha | q) + E_c(\beta; \beta | q) + 2E_c(\alpha; \beta | q)$$

should be the same at  $q=(000)$  along  $[100]$  and  $[111]$  direction in  $\mathbf{k}$  space. Thus, the crystallographic requirements impose severe constraints on the wave-vector-magnitude dependence of the CEE modulus.

The CEE modulus shown in Fig. 4 exhibits several significant characteristics; strong orientation and wave-vector-magnitude dependence are indicated in the contour maps of elastic energy moduli. The pronounced anisotropy of the CEE modulus especially is observed at the origin of  $\mathbf{k}$  space. In Fig. 4(a), the value  $e_{100}(+)$  is  $6.42 \times 10^{-21}$  J/atom but  $e_{110}(+)$  is  $11.2 \times 10^{-21}$  J/atom at the origin of  $\mathbf{k}$  space. Similarly, the anisotropy is shown at the origin in Fig. 4(c) as  $e_{100}(-) = -12.7 \times 10^{-21}$  J/atom and  $e_{110}(-) = 1.89 \times 10^{-21}$  J/atom. Referring to the sign of the cross term

$E_c(\alpha; \beta | q)$  shown in Fig. 1(b), the acoustic branches of the CEE moduli along the high-symmetry directions are shown in Fig. 5(a). At the origin of  $\mathbf{k}$  space, the CEE moduli  $e_{100}(-)$ ,  $e_{110}(+)$ , and  $e_{111}(+)$  are the values corresponding to  $2\Omega\eta^2[Y(q) - \langle Y(q) \rangle]$  along  $\langle q \rangle = \langle 100 \rangle$ ,  $\langle 110 \rangle$ , and  $\langle 111 \rangle$  directions, respectively, in the expression used by Cahn in his continuum model.<sup>1</sup> These values are in the order of  $e_{100}(-) < e_{110}(+) < e_{111}(+)$  as usually expected in metal alloys. Figure 5(b) shows the optical branches of the CEE moduli of the  $\beta$ -brass. As mentioned above, the optical mode of decomposition waves with the wave vector  $q=(0,0,0)$  represents ordering waves. For example, the optical waves with  $q=(0,0,0)$  along  $[100]$  direction give rise to a more perfect  $B2$  phase (cf. Fig. 3). It is to be noted, however, that the amplitude of the waves on the  $\alpha$  sublattice may be different in its magnitude from that on the  $\beta$  sublattice. In fact, those associated with the negative eigenvalue of the  $B2$  ordering are asymmetrical with respect to the average concentration  $c$ . Hence, strictly speaking, the ordering of the  $B2$  phase is not described by a single parameter but it should be described by using two long-range-order parameters which represent the amplitudes of the waves on the  $\alpha$  and

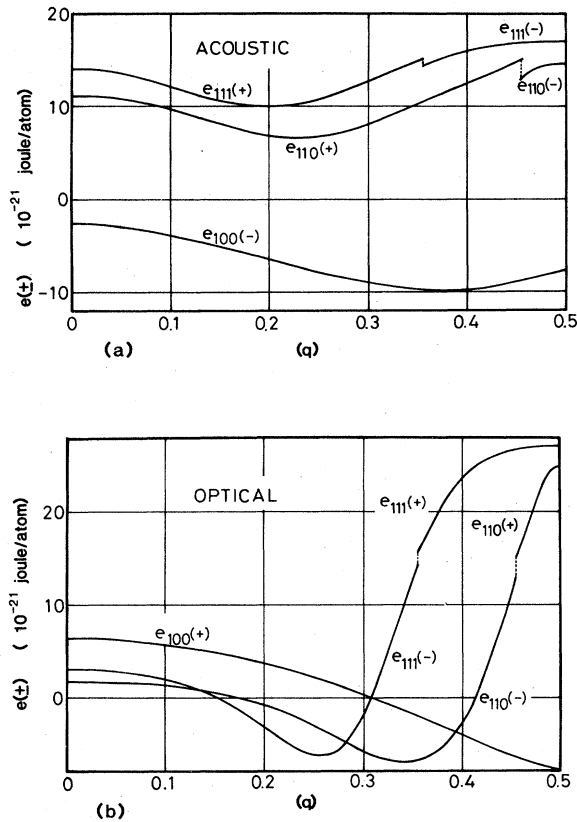


FIG. 5. (a) Acoustic branches of the CEE moduli are shown along high symmetric directions in  $\mathbf{k}$  space. (b) The optical branches of CEE in  $\beta$ -brass, where the waves with the wave vector  $\underline{k}(q) = \underline{k}(0,0,0)$  indicate ordering waves.

the  $\beta$  sublattice.

The curves  $e_{110}(\pm)$  and  $e_{111}(\pm)$  in Figs. 5(a) and 5(b) exhibit characteristic features. The moduli  $e_{110}(-)$  and  $e_{110}(+)$  which have the values  $1.89 \times 10^{-21}$  J/atom and  $11.2 \times 10^{-21}$  J/atom at the origin, respectively, have energy gaps at the point  $(q) = (0.45, 0.45, 0)$ . This is originated in the variation of  $E_c(\alpha; \beta | q)$  with the wave vector  $\underline{k}(q)$ . Corresponding to the variation of  $E_c(\alpha; \beta | q)$  with  $\underline{k}(q)$ , the eigenvectors  $\underline{Q}(\pm)$  change their directions in  $Q_\alpha - Q_\beta$  space. For example, the eigenvector  $\underline{Q}(-)$  located in the region  $Q_\alpha Q_\beta < 0$  at  $q = (0,0,0)$  rotates clockwise with the increase of the wave vector  $\underline{k}(q, q, 0)$  and coincides with the  $Q_\alpha$  axis at the point  $(q)_g = (0.45, 0.45, 0)$ , where the modulus  $E_c(\alpha; \beta | q)$  vanishes and the eigenvalue  $e(-)$  has the value  $E_c(\alpha; \alpha | q)$ . Because this wave takes place only on the  $\alpha$  sublattice, i.e., zero-amplitude on the  $\beta$  sublattice, it can be either optical or acoustic. On the other hand, the eigenvector  $\underline{Q}(+)$  which coincides with the  $\beta$  sublattice at  $(q)_g$  exhibits the eigenvalue  $e(+) = E_c(\beta; \beta | q)$ . Thus, either the optical or the acoustic wave with the wave vector  $\underline{k}(q)_g$  can have the different eigenvalues  $e(-) = E_c(\alpha; \alpha | q)$  and  $e(+) = E_c(\beta; \beta | q)$  as shown in Fig. 5, that is, the energy gaps appear at the point  $(q)_g$ . Hence, over the point  $(q)_g$ , the eigenvector  $\underline{Q}(-)$  moves into the region  $Q_\alpha Q_\beta > 0$ . The eigenvalue

$e_{110}(+)$  is, therefore, plotted on the right-hand side of  $e_{110}(-)$  as shown in Fig. 5(a). The similar features are observed on the curves  $e_{111}(\pm)$  in Figs. 5(a) and 5(b). It is to be noted that the modulus  $E_c(\alpha; \beta | q)$  also changes the sign across the point  $(q) = (0.36, 0.36, 0.36)$  as shown in Fig. 1(e).

The theory predicts that the wave with the wave vector  $(q) = (\frac{1}{2}, \frac{1}{2}, \frac{1}{2})$  cannot grow up, because both values of  $e(\pm)$  have positive values at that position. Since this wave is an ordering wave which makes  $DO_3$  structure from a  $B2$  structure, the elastic energy evidently works in a manner that depresses the  $DO_3$  ordering. Figure 6 indicates the  $DO_3$  ordering waves on the  $\alpha$  and the  $\beta$  sublattice having a wavelength equal to  $2a/\sqrt{3}$  the  $[111]$  direction. The solid curve on the  $\beta$  sublattice gives rise to the maximum CEE and the dashed curve gives the minimum CEE. Only the amplitudes of the two waves on the  $\beta$  sublattice are essential with respect to the CEE for forming a  $DO_3$  phase, because the sinusoidal composition waves represented by the solid and the dashed curves in Fig. 6 would give the same crystal if the amplitudes were the same. The ratio of the amplitude of the waves on the  $\alpha$  sublattice to that of the broken curve and to that of the solid curve on the  $\beta$  sublattice is given by 1:0.6:1.7.

The point  $(\frac{1}{2}, \frac{1}{2}, \frac{1}{2})$  is a special point of bcc structure where two or more symmetry elements of the point group of the disordered phase intersect. Therefore, the vector representing the gradient  $\nabla V(q)$  of an arbitrary potential energy  $V(q)$  must vanish at the special point. At present, putting  $V(q)$  equal to  $e_{111}(+)$  or  $e_{111}(-)$ , we find that the values  $e_{111}(\pm)$  must present extrema regardless of the choice of CP's. By this reason, they have the maximum values at the point  $(q) = (\frac{1}{2}, \frac{1}{2}, \frac{1}{2})$  as shown in Fig. 5. On the other hand, the other curves in the figures may be inclined at the points on the BZ boundary, because they are not special points.

#### IV. SUMMARY AND DISCUSSION

The microscopic elasticity theory has been used to consider the role of the CEE in the ordered phase on the con-

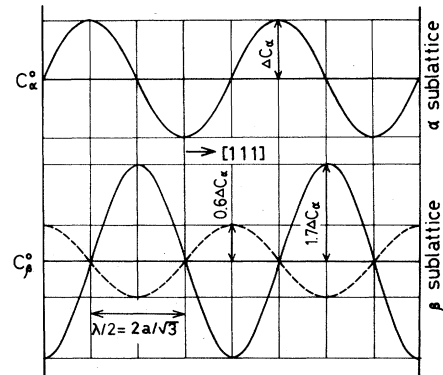


FIG. 6. Schematic drawing of  $DO_3$  ordering waves in a  $B2$ -type ordered phase with the wavelength  $2a/\sqrt{3}$  along the  $[111]$  direction. The relative amplitude shown is the one estimated from the configurational elastic energy of  $\beta$ -brass. Either the solid curve or the dashed curve on the  $\beta$  sublattice takes part in forming the  $DO_3$  phase with the wave on the  $\alpha$  sublattice.



tinuous clustering and order-disorder transition. The theory is applied to the  $\beta$ -brass, because all of the CP's necessary for calculating the CEE have been obtained from experiments. The results have been stated in terms of the CEE moduli  $E_c(\gamma; \gamma' | q)$ 's and the eigenvalues  $e(\pm)$ . The direction of the eigenvectors in the amplitude space argues that the sign of the modulus  $E_c(\alpha; \beta | q)$  determines the phase angle difference between the waves on the  $\alpha$  and the  $\beta$  sublattice in the limit of very long wavelength. As a consequence, two different modes of decomposition waves, i.e., optical and acoustic mode of waves, are found to be associated with the maximum and

the minimum elastic energies. The phase angle of the decomposition waves have been considered intuitively on the analogy of lattice dynamics. However, strictly speaking, since the decomposition wave treats the concentration of atoms and the lattice dynamics is concerned with the atom displacements, they have nothing to do with each other. Therefore, the results derived intuitively about the phase difference of the decomposition waves should be considered strictly. The single wave with the wave vector  $\underline{k}(q)$  is taken into account for simplicity. Then, the concentration variance  $\Delta c(n\gamma)$  is expressed as follows:

$$\Delta c(n\gamma) = Q(\gamma | q) \cos[2\pi(n_1 q \pm \delta)] \cos[2\pi(n_2 q \pm \delta)] \cos[2\pi(n_3 q \pm \delta)], \quad (11a)$$

$$\delta = \begin{cases} \frac{1-q}{2} & \text{(optic branch) and } \frac{q}{2} & \text{(acoustic branch) for } \beta\text{-sublattice,} \\ 0 & \text{for } \alpha\text{-sublattice,} \end{cases} \quad (11b)$$

$$(11c)$$

where the  $\pm\delta$  indicates that the  $\beta$  sublattice position can be expressed in terms of either way given by  $\underline{x}(n\beta) = \underline{x}(n) \pm \underline{x}(\frac{1}{2}, \frac{1}{2}, \frac{1}{2})$ . The phase difference  $\delta$  has two different values expressed as  $(1-q)/2$  and  $q/2$  according to the optical and the acoustic branches of the CEE moduli, respectively. That is, the one wave vector  $\underline{k}(q)$  represents two different modes of decomposition waves. The amplitude  $Q(\gamma | q)$  is assumed to be real in the above expression. We consider first the wave with the wave vector  $\underline{k}(q) = \underline{k}(\frac{1}{2}, \frac{1}{2}, \frac{1}{2})$  as a representative point on the BZ boundary. It is clear from Eq. (11b) that the phase difference  $\delta$  between the waves on the  $\alpha$  and  $\beta$  sublattice is  $\pi/2$ . Therefore, two possible concentration waves can be drawn on the  $\beta$  sublattice as shown in Fig. 6. The dashed curve exhibits the  $\pi/2$  phase difference and the solid curve gives the  $-\pi/2$  phase difference with respect to the concentration wave on the  $\alpha$  sublattice. Both concentration waves give the same  $DO_3$  structure, and only the amplitudes are significant on the transition. With decreasing  $q$ , both curves on the  $\beta$  sublattice shift toward the left-hand side relative to the curve on the  $\alpha$  sublattice, according to the phase difference  $+\delta$ . Consequently, in this case the phase difference increases with the dashed curve as indicated by the expression  $\delta = (1-q)/2$ , but it decreases with the solid curve in proportion to  $\delta = q/2$ . In the limit of long wavelength, the dashed curve has the phase difference given by  $\pi$  with respect to the concentration wave on the  $\alpha$  sublattice and the solid curve has no phase difference. On the contrary, according to the phase difference  $-\delta$ , both curves on the  $\beta$  sublattice shift relatively toward the right-hand side with decreasing  $q$ . Consequently, the concentration waves with a wave vector  $\underline{k}(q)$  have four different phase angles between the origin and the point on the BZ boundary in  $\mathbf{k}$  space. The solid curve shifted by the angle  $-2\pi\delta$  should exhibit the phase difference  $-\pi$  in the limit of very long wavelength and the dashed curve should show no phase difference there. This configuration of concentration waves is identical to that mentioned above in connection with the plus sign of

the phase difference. Thus, it is evident that the concentration waves in the ordered phase can be treated in the same way as the displacement waves in the theory of lattice dynamics.

The role of the CEE on the transition can be made clear by taking the total free energy into account. The pairwise chemical interchange energies of the  $\beta$ -brass are obtained by Inden<sup>35</sup> to the second neighbor of atoms:

$$\omega^{(1)} = -320k_B, \quad \omega^{(2)} = -180k_B,$$

where  $k_B$  is the Boltzmann constant. The above numerical values are those obtained by Inden but multiplied by  $-\frac{1}{2}$  to conform our definition of interchange energy  $\omega = v_{ij} - (v_{ii} + v_{jj})/2$  where the symbols  $v_{ij}$  indicate binding energy between  $i$  and  $j$  species of atoms. The sign of the interchange energy  $\omega^{(1)}$  signifies that the  $B2$  phase is stable below the critical temperature  $T_c$  for  $B2$  ordering and  $\omega^{(2)}$  indicates that the  $DO_3$  ordering takes place in the  $B2$  phase. In fact, Inden<sup>35</sup> has drawn the stable region of  $DO_3$  phase in his calculated equilibrium phase diagram. However, no  $DO_3$  ordering in a  $\beta$ -brass has been reported. This contradiction is thought to be caused by the neglect of the CEE contribution in his calculation. To discuss this problem, the Fourier transform of the configurational chemical free energy (CEE)  $\Omega(\gamma; \gamma' | q)$  is considered. The general form of  $\Omega(\gamma; \gamma' | q)$  in a  $\beta$ -brass has been given in Ref. 33. Calculation of CCE moduli is made on the  $\beta$ -brass with  $\eta = 0.5c$  at  $100^\circ\text{C}$  which is the condition that the spinodal decomposition takes place in the  $\beta$ -brass with  $c = 0.389$ .<sup>29</sup> By using the CCE moduli estimated, the eigenvalue  $\Omega(-)$  of the moduli can be obtained as shown in Fig. 7. The contour map of  $\Omega(+)$  which shows mostly optical modes of decomposition is omitted here, because it is not important for the present discussion of the CEE effect on the total free energy of  $\beta$ -brass. A negative region of the CEE appears around the origin and around the point  $(q) = (\frac{1}{2}, \frac{1}{2}, \frac{1}{2})$  in Fig. 7. The wave vectors around the origin indicate the waves for spinodal decomposition

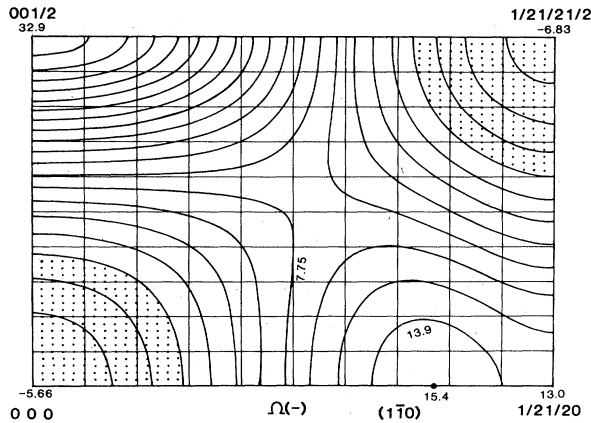


FIG. 7. Eigenvalue contours  $\Omega(-)$  of configurational chemical energy modulus in  $\beta$ -brass in units of  $10^{-21}$  J/atom.

and the wave vector  $(q) = (\frac{1}{2}, \frac{1}{2}, \frac{1}{2})$  indicates the  $D0_3$  ordering. Neglecting the entropy term, we can obtain  $\Omega(-) = 8\omega^{(1)} + 6\omega^{(2)}$  at  $(q) = (0,0,0)$  and  $\Omega(-) = 12\omega^{(2)}$  at  $(q) = (\frac{1}{2}, \frac{1}{2}, \frac{1}{2})$ . By adding the CCE  $\Omega(\gamma; \gamma' | q)$  to the CEE  $E_c(\gamma; \gamma' | q)$ , we can obtain the eigenvalues  $f(\pm)$  of the total-energy moduli. Figure 8 shows the view of the contour of  $f(-)$  which is pertinent to the present discussion. It is to be noted that the negative region that appeared around  $(q) = (\frac{1}{2}, \frac{1}{2}, \frac{1}{2})$  in the CCE moduli (Fig. 7) has disappeared in Fig. 8. This is the consequence of the elastic energy effect shown in Fig. 4(d). That is the CEE works in a manner that depresses the  $D0_3$  ordering in a  $\beta$ -brass. On the other hand, it is clear from Fig. 4(d) and

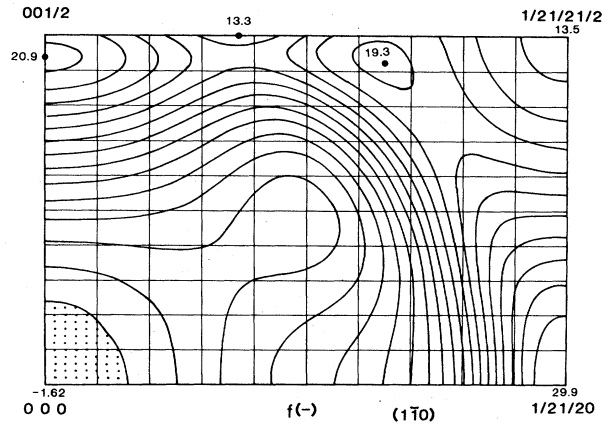


FIG. 8. View of the eigenvalue contours  $f(-)$  of total (chemical plus elastic) configurational free-energy modulus in  $\beta$ -brass in units of  $10^{-21}$  J/atom.

Fig. 8 that the CEE works by assisting the spinodal decomposition in a  $\beta$ -brass. Thus, the contribution of the CEE is found to be essential on the diffusional transition in the  $\beta$ -brass.

#### ACKNOWLEDGMENTS

The author wishes to express his gratitude to Professor C. M. Wayman, University of Illinois, for many valuable discussions and a critical review of this paper. Thanks are due to Dr. H. Okada, Nippon Steel Corporation, for support on this study and for his encouragement; and to Dr. M. Kama for his help on the computer calculation.

- <sup>1</sup>J. W. Cahn, *Acta Metall.* **9**, 795 (1961); **10**, 179 (1962).
- <sup>2</sup>T. Matsubara, *J. Phys. Soc. Jpn.* **7**, 270 (1952).
- <sup>3</sup>H. Kanzaki, *J. Phys. Chem. Solids* **2**, 24 (1957); **2**, 107 (1957).
- <sup>4</sup>M. A. Krivoglaz and E. A. Tikhonova, *Ukr. Fiz. Zh. (Russ. Ed.)* **3**, 297 (1958).
- <sup>5</sup>A. G. Khachatryan, *Kristallografiya* **10**, 303 (1965) [*Sov. Phys. Crystallogr.* **10**, 246 (1965)].
- <sup>6</sup>A. G. Khachatryan, *Fiz. Tverd. Tela (Leningrad)* **4**, 2840 (1963) [*Sov. Phys.—Solid State* **4**, 2081 (1963)].
- <sup>7</sup>H. E. Cook and D. de Fontaine, *Acta Metall.* **17**, 915 (1969); **19**, 607 (1971).
- <sup>8</sup>G. L. Krasko, *Phys. Rev. B* **26**, 4389 (1982).
- <sup>9</sup>A. G. Khachatryan, *Fiz. Met. Metalloved.* **13**, 493 (1962) [*Phys. Met. Metallogr. (USSR)* **13**, 493 (1963)].
- <sup>10</sup>A. G. Khachatryan, *Fiz. Tverd. Tela (Leningrad)* **5**, 26 (1963) [*Sov. Phys.—Solid State* **5**, 16 (1963)].
- <sup>11</sup>D. de Fontaine and H. E. Cook, *Battelle Colloquium on Critical Phenomena* (Gstaad, Switzerland, 1971), pp. 257–275.
- <sup>12</sup>D. de Fontaine, *Acta Metall.* **21**, 553 (1973).
- <sup>13</sup>A. G. Khachatryan, in *Progress in Materials Science*, edited by B. Chalmers, J. W. Christian, and T. B. Massalski (Pergamon, New York, 1979), Vol. 22, pp. 1–151.
- <sup>14</sup>T. Kajitani and H. Cook, *Acta Metall.* **26**, 1371 (1978).
- <sup>15</sup>H. E. Cook, *Acta Metall.* **23**, 1027 (1975); **23**, 1041 (1975).
- <sup>16</sup>H. E. Cook, *Acta Metall.* **21**, 1431 (1973).
- <sup>17</sup>M. Suezawa and H. Cook, *Acta Metall.* **26**, 1205 (1978).
- <sup>18</sup>M. Suezawa, *Trans. Jpn. Inst. Met.* **19**, 459 (1978).
- <sup>19</sup>W. Köster, *Z. Metallkd.* **32**, 145 (1940).
- <sup>20</sup>G. M. McManus, *Phys. Rev.* **129**, 2004 (1963).
- <sup>21</sup>H. Kubo and C. M. Wayman, *Metall. Trans.* **10A**, 633 (1979).
- <sup>22</sup>H. Kubo, I. Cornelis, and C. M. Wayman, *Acta Metall.* **28**, 405 (1980).
- <sup>23</sup>S. M. Allen and J. W. Cahn, *Acta Metall.* **20**, 423 (1972); **23**, 1017 (1975); **24**, 425 (1976).
- <sup>24</sup>H. Ino, *Acta Metall.* **26**, 827 (1978).
- <sup>25</sup>V. Paider, *Czech. J. Phys. B* **27**, 50 (1977).
- <sup>26</sup>V. Paider, *Phys. Status Solidi A* **21**, K73 (1974).
- <sup>27</sup>G. Inden and P. Wolfgang, *Z. Metallkd.* **62**, 627 (1971).
- <sup>28</sup>H. Warlimont, *Z. Metallkd.* **59**, 598 (1968).
- <sup>29</sup>H. Kubo, *Trans. Jpn. Inst. Met.* **23**, 655 (1982).
- <sup>30</sup>G. Gilat and G. Dolling, *Phys. Rev.* **138**, A1053 (1965).
- <sup>31</sup>T. B. Wu, in *Proceedings of the International Conference on Phase Transformation in Solids*, June, 1983, Crete, Greece (unpublished).
- <sup>32</sup>H. Cook, *J. Phys. Chem. Solids* **30**, 1097 (1969).
- <sup>33</sup>H. Kubo, *J. Phys. Chem. Solids* **44**, 323 (1983).
- <sup>34</sup>M. Born and K. Huang, *Dynamical Theory of Crystal Lattices* (Oxford University Press, Oxford, 1954).
- <sup>35</sup>G. Inden, *Z. Metallkd.* **66**, 648 (1975).